Hindawi Publishing Corporation
Mathematical Problems in Engineering
Volume 2013, Article ID 313197, 11 pages
http://dx.doi.org/10.1155/2013/313197

Research Article

Optimal Ascent Guidance for Air-Breathing Launch Vehicle Based on Optimal Trajectory Correction

Xuefang Lu, Yongji Wang, and Lei Liu

Key Laboratory of Ministry of Education for Image Processing and Intelligent Control, School of Automation, Huazhong University of Science and Technology, Wuhan 430074, China

Correspondence should be addressed to Yongji Wang; wangyjch@mail.hust.edu.cn

Received 14 October 2013; Revised 28 October 2013; Accepted 28 October 2013

Academic Editor: Hui Zhang

An optimal guidance algorithm for air-breathing launch vehicle is proposed based on optimal trajectory correction. The optimal trajectory correction problem is a nonlinear optimal feedback control problem with state inequality constraints which results in a nonlinear and nondifferentiable two-point boundary value problem (TPBVP). It is difficult to solve TPBVP on-board. To reduce the on-board calculation cost, the proposed guidance algorithm corrects the reference trajectory in every guidance cycle to satisfy the optimality condition of the optimal feedback control problem. By linearizing the optimality condition, the linear TPBVP is obtained for the optimal trajectory correction. The solution of the linear TPBVP is obtained by solving linear equations through the Simpson rule. Considering the solution of the linear TPBVP as the searching direction for the correction values, the updating step size is generated by linear search. Smooth approximation is applied to the inequality constraints for the nondifferentiable Hamiltonian. The sufficient condition for the global convergence of the algorithm is given in this paper. Finally, simulation results show the effectiveness of the proposed algorithm.

1. Introduction

The development of space technology has given rise to the expectation that launchers will become low cost and fully reusable. The launch vehicle with hypersonic air-breathing propulsion is considered to reduce the cost of payloads taken to the Earth's orbit. The air-breathing launch has inherent features that make it a candidate for future space transportation [1]. The impulse of air-breathing propulsion, which is approximately 3000 s [2], is significantly higher than that of a rocket (360 s). Air-breathing propulsion brings high impulse as well as strong nonlinear, coupling aerodynamic and thrust.

The traditional design category for ascent guidance is to drive an optimal nominal trajectory off-board. The guidance problem is then transformed into a tracking problem for the designed optimal nominal trajectory. The design of a trajectory could be formulated as a global optimization task [3]. The methods for numerical optimization of continuous dynamic systems could be termed "Hamiltonian" (indirect method) and "Transcription" (direct method) [4]. For the optimization problem with inequality constraints, smoothing approximation was considered in [5, 6]. A filled function approach for nonsmooth constrained global optimization was presented in [7]. Linear-quadratic optimization was implemented to optimal control in [8]. Direct and indirect optimization methods were implemented to the off-board trajectory optimization problem in previous literature. The numerical algorithms of trajectory optimization for vehicles were summarized and systematically analyzed in [9, 10]. A new concept of pseudocontrol sets to solve optimal control problems was proposed in [11]. This approach reduces the calculation cost by combining large-scale linear programming algorithms with discretization of the continuous system dynamics on small segments. An algorithm for multiobjective optimization was presented in [12]. Intelligent algorithms can also be used for trajectory optimization problems. The particle swarm optimization (PSO) method was implemented to the space trajectory optimization in [13]. The simulation results showed the effective of PSO in finding the optimal solution to the space trajectory optimization problems, with great numerical accuracy. Approximate numerical methods

of optimization were presented for multiorbit noncoplanar orbit transfers of low-thrust spacecraft in [14].

Many control methods were implemented to trajectory tracking guidance and control problem [15]. In the previous literature, many researchers focused on the robust control method [16, 17]. It has obtained successful application in the industry [18, 19]. For the networked control system, a H-infinity step tracking control method was presented in [20]. An adaptive fuzzy robust control for a class of nonlinear systems was proposed in [21]. An adaptive guidance law and off-board trajectory optimization for air-breathing launch vehicle were addressed in [22]. In that paper, the optimal control problem was solved using SQP method. And the adaptive guidance law was developed using a feedback loop based on a second-order rate controller for angle of attack. A robust state feedback guidance law was generated in real time using the indirect Legendre pseudospectral feedback method in [23]. In that paper, the guidance problem was converted into a trajectory state regulation problem which is a linear time varying system.

However, the accuracy of the trajectory tracking method is low with the disturbance and the modeling error. It lacks the autonomy and adaptability to cope with the non-nominal vehicle and mission conditions needed for future reusable launch vehicles [24]. To improve the performance and the accuracy of the guidance, the optimal guidance method generates the prospective trajectory by fast trajectory optimization on-board based on current flight state. This guidance method has become a research focus with the advance in on-board computation capability. Ping Lu used the indirect method to pose the trajectory optimization problem as a nonlinear two-point boundary value problem (TPBVP) in [25, 26]. From this model, the optimal thrust vector that satisfied the optimality condition was derived. A finite difference method was employed to solve the nonlinear TPBVP through numerical calculations. Similarly, a fast trajectory optimization for hypersonic air-breathing vehicles was presented in [27]. The indirect method was implemented for ascent trajectory optimization on-board considering the features of the air-breathing vehicle. Ping Lu's work is significant for the optimal ascent guidance. However, the TPBVP is nonlinear and nondifferentiable for the air breathing launch vehicle. It is difficult to solve the nonlinear and nondifferentiable TPBVP on-board in every guidance cycle. Using the direct method, a new guidance concept based on nonlinear programming (NLP) method was proposed in [24]. NLP-based guidance concepts appear advantageous over conventional methods because the on-board guidance algorithm allows a single algorithm to be implemented for different vehicles and missions. The optimal control problem was parameterized into a nonlinear programming problem that was solved by the gradient projection algorithm. In [28], the reference trajectory was updated for disturbance by an on-board algorithm that satisfied the real-time requirement. A new real-time guidance method derived from the optimality condition was proposed in [29]. In that paper, the simple guidance parameters were updated in real time. In [30], a guidance method was presented for online launcher ascent trajectory updating based on neural networks. In the paper, the utilization of a neural network approximation was used online during the ascent flight, with a training process performed off-line.

In this paper, we present an optimal guidance algorithm for air breathing launch vehicle based on optimal trajectory correction to reduce the on-board calculation cost. Considering the current vehicle state as the initial condition, the optimal trajectory correction problem is referred to as a nonlinear optimal control problem with state inequality constraints. For the real-time requirement of the on-board algorithm, the linear TPBVP is obtained for optimal trajectory correction by linearizing the optimality condition in this paper. The Simpson rule is applied to transform the linear TPBVP into linear equations. Considering the solution of the linear TPBVP as the searching direction for the correction values, the updating step size is generated by linear search. Smooth approximation is applied to the inequality constraints for the nondifferentiable Hamiltonian. The sufficient condition for the global convergence of the algorithm is given in this paper. Finally, simulation results for different cases of the modeling error show the effectiveness of the proposed algorithm. In summation, the main contributions of this paper are given as follows.

(1) We reduce the on-board calculation cost of the guidance method a lot. Comparing with the methods in previous literatures which solves nonlinear equations in every guidance cycle, the proposed guidance method in this paper solves linear equations once in every guidance cycle only.

(2) We obtain the relationship between the global convergence and the guidance cycle of the online algorithm. The sufficient condition of the global convergence of this algorithm is given.

The remainder of this paper is organized as follows. Section 2 presents the state normalized-energy differential equations of motion of the vehicle and the optimal control problem for optimal ascent guidance. Section 3 provides details on the optimal guidance algorithm. Section 4 presents an analysis of the global convergence of the proposed algorithm. Section 5 discusses the proposed differentiable approximation for Hamiltonian. Section 6 presents the simulations for the Generic Hypersonic Vehicle (GHV) model and scramjet engine. Section 7 presents the conclusion.

2. Problem Formulation

2.1. Ascent Dynamic. The formulation of motion of the air-breathing vehicle in the longitudinal plane is presented in this section. As shown in Figure 1, the thrust T, gravitation g, and the aerodynamic lift force L and drag force D are acting on the vehicle. The angle of attack α is the angle between the body axis and the vector of the velocity v. The flight path angle γ is the angle between the vector of the velocity v and the ground plane.

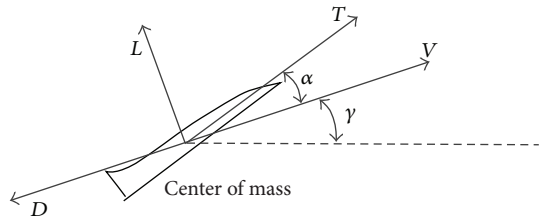

Figure 1: The forces acting on the vehicle.

The motion of the vehicle in the longitudinal plane can be described as follows:

$$\begin{aligned}
\frac{dr}{dt} &= v\sin\gamma,\\
\frac{dv}{dt} &= \frac{T\cos\alpha - D}{m} - g\sin\gamma,\\
\frac{d\gamma}{dt} &= \frac{1}{v}\left[\frac{T\sin\alpha + L}{m}\cos\sigma - g\cos\gamma + \frac{v^2}{r}\cos\gamma\right],\\
\frac{dm}{dt} &= -\frac{T}{I_{\mathrm{sp}}},
\end{aligned} \tag{1}$$

where r, m, I_{sp}, and g are the altitude, weight of the vehicle, impulse, and gravity acceleration, respectively.

The lift force L and the drag force D are given as follows:

$$\begin{aligned}
L &= \frac{1}{2}\rho v^2 S_{\mathrm{ref}} C_L\left(M_a, \alpha\right),\\
D &= \frac{1}{2}\rho v^2 S_{\mathrm{ref}} C_D\left(M_a, \alpha\right),
\end{aligned} \tag{2}$$

where ρ and S_{ref} are the air density of the current altitude and the reference area respectively, C_L and C_D are the lift coefficient and the drag coefficient, respectively, which are the nonlinear functions of the angle of attack α and Mach number M_a. For the air-breathing engine, the thrust is given by

$$T = T\left(\rho, M_a, \alpha, \phi\right), \tag{3}$$

where T is the nonlinear function of ρ, α, M_a, and the throttle command ϕ.

In [25], the equations were normalized to reduce the numerical calculation error. Variable substitutions are applied as follows:

$$R = \frac{r}{r_0}, \qquad V = \frac{v}{\sqrt{g_0 r_0}}, \qquad g = \frac{g_0 r_0^2}{r^2}, \tag{4}$$

where r_0 and g_0 are Earth radius and the ground gravity acceleration, respectively. Considering the thrust T and aerodynamic forces as a composition of forces, we define the normalized accelerations a_T and a_L as follows:

$$a_T = \frac{T\cos\alpha - D}{m g_0}, \qquad a_L = \frac{T\sin\alpha + L}{m g_0}. \tag{5}$$

We define

$$\tau = \frac{t}{\sqrt{r_0/g_0}}. \tag{6}$$

The normalized equations of motion are obtained from (1), (4), (5), and (6) as follows:

$$\begin{aligned}
\frac{dR}{d\tau} &= V\sin\gamma,\\
\frac{dV}{d\tau} &= a_T - \frac{\sin\gamma}{R^2},\\
\frac{d\gamma}{d\tau} &= \frac{1}{V}\left[a_L + \left(V^2 - \frac{1}{R}\right)\left(\frac{\cos\gamma}{R}\right)\right],\\
\frac{dm}{d\tau} &= -\frac{T\sqrt{r_0}}{I_{\mathrm{sp}}\sqrt{g_0}}.
\end{aligned} \tag{7}$$

The mission of ascent is to send the vehicle to the required final state which is denoted as (R_f, V_f, γ_f). Define normalized-energy E as follows:

$$E = \frac{V^2}{2} - \frac{1}{R}. \tag{8}$$

From (8) we obtain

$$\begin{aligned}
\frac{dE}{d\tau} &= V a_T,\\
\frac{dR}{dE} &= \frac{\sin\gamma}{a_T},\\
\frac{dV}{dE} &= \frac{1}{a_T V}\left[a_T - \frac{\sin\gamma}{R^2}\right],\\
\frac{d\gamma}{dE} &= \frac{1}{a_T V^2}\left[a_L + \left(V^2 - \frac{1}{R}\right)\left(\frac{\cos\gamma}{R}\right)\right],\\
\frac{dm}{dE} &= -\frac{T\sqrt{r_0}}{a_T V I_{\mathrm{sp}}\sqrt{g_0}}.
\end{aligned} \tag{9}$$

The integration interval $[E_0, E_f]$ is fixed.

2.2. Optimal Feedback Control Problem for Ascent Guidance. In this section, the optimal feedback control problem for optimal ascent guidance is addressed. This problem differs from trajectory optimization off-board in that the initial state of the optimal control problem is obtained from the navigation system. We denote the state and the guidance command of the trajectory as

$$\begin{aligned}
x(E) &= \left[R(E) \;\; V(E) \;\; \gamma(E) \;\; m(E)\right]^T,\\
u(E) &= \left[\alpha(E) \;\; \phi(E)\right]^T.
\end{aligned} \tag{10}$$

With the feedback vehicle state xc_k obtained from navigation system, the optimal ascent guidance algorithm is used to

generate new reference trajectory $[x(E)\ \ u(E)]^T$ and output $u(E)$ from the following optimal control problem:

$$\begin{aligned} \min\quad & J = \phi\left(x\left(E_f\right)\right) + \int_{Ec_{k+1}}^{E_f} g\left(x,u\right) dE, \\ \text{s.t.}\quad & \dot{x} = f\left(x,u\right), \\ & x\left(Ec_k\right) = xc_k, \\ & W\left(x\left(E_f\right)\right) = 0, \\ & C\left(x,u\right) \le 0, \end{aligned} \tag{11}$$

where Ec_k is the normalized energy for current vehicle state xc_k.

3. Optimal Ascent Guidance Algorithm

In [25, 26], the optimal control problem was solved on-board in every guidance cycle. However, it is difficult to solve the nonlinear and nondifferentiable TPBVP on-board for air-breathing launch vehicles. In this section, we propose an optimal guidance algorithm. This guidance algorithm updates the reference trajectory $[x\ \ u]^T$ in every guidance cycle to deal with the unknown disturbance. For the current state xc_k of the kth guidance cycle, the optimal feedback control problem is transformed into a linear TPBVP problem using optimality condition linear approximation. The searching direction of the correction values d_k is obtained by solving the linear TPBVP. With the searching direction, the new reference trajectory is generated by linear search. For the kth guidance cycle, the trajectory update is performed as follows:

$$\left[x_{k+1}(E)\ \ u_{k+1}(E)\right]^T = \left[x_k(E)\ \ u_k(E)\right]^T + l_k d_k^T(E). \tag{12}$$

The initial reference trajectory $[x_0(E)\ \ u_0(E)]^T$ is derived from the off-board from trajectory optimization by direct method. The flow chart of the algorithm is shown in Figure 2. Figure 3 shows the time sequence of algorithm.

3.1. Linear Approximation for the Optimality Condition. In this section, we linearize the optimality condition for optimality trajectory updating. The optimal control problem (11) without inequality constraints is given as follows:

$$\begin{aligned} \min\quad & J = \phi\left(x\left(E_f\right)\right) + \int_{Ec_{k+1}}^{E_f} g\left(x,u\right) dE, \\ \text{s.t.}\quad & \dot{x} = f\left(x,u\right), \\ & x\left(Ec_k\right) = xc_k, \\ & W\left(x\left(E_f\right)\right) = 0. \end{aligned} \tag{13}$$

The Hamiltonian of (13) is given as follows:

$$H = g\left(x,u\right) + \lambda^T f\left(x,u\right), \tag{14}$$

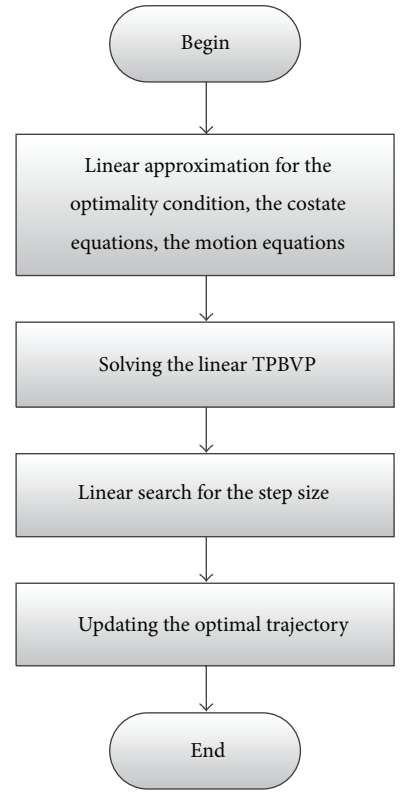

Figure 2: Flow chart of the optimal ascent guidance algorithm.

where λ is the costate vector. The state equations, costate equations, and optimality condition for the optimal control problem are given by

$$\begin{aligned} \dot{x} &= f\left(x,u\right), \\ \dot{\lambda} &= -\left(\frac{\partial H}{\partial x}\right)^T, \\ \frac{\partial H}{\partial u} &= 0. \end{aligned} \tag{15}$$

The initial and transversality conditions are given by

$$\begin{aligned} x\left(Ec_k\right) &= xc_k, \\ W\left(x\left(E_f\right)\right) &= 0, \\ \lambda\left(E_f\right) &= \left[\frac{\partial \phi}{\partial x\left(E_f\right)}\right]^T + \left[\varpi^T \frac{\partial W}{\partial x\left(E_f\right)}\right]^T. \end{aligned} \tag{16}$$

We denote the trajectory correction variables as follows:

$$\begin{bmatrix} \Delta x\left(E\right) \\ \Delta u\left(E\right) \\ \Delta \lambda\left(E\right) \end{bmatrix} = \begin{bmatrix} x\left(E\right) - x_k\left(E\right) \\ u\left(E\right) - u_k\left(E\right) \\ \lambda\left(E\right) - \lambda_k\left(E\right) \end{bmatrix}. \tag{17}$$

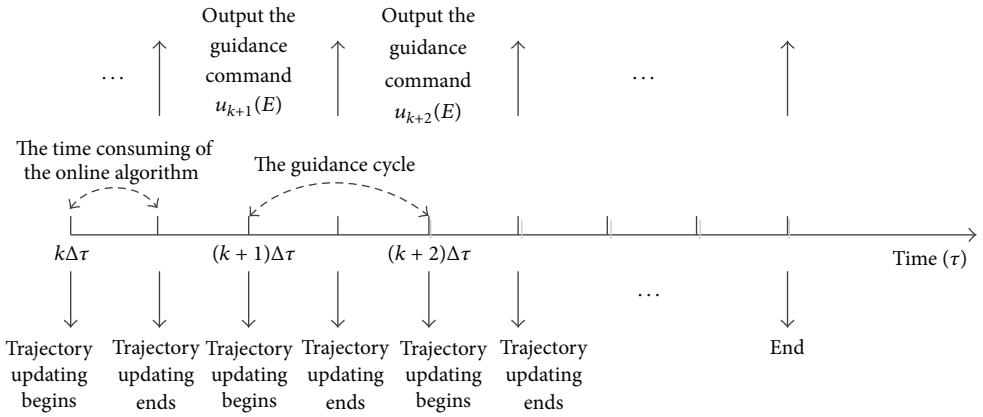

Figure 3: Time sequence of the optimal ascent guidance algorithm.

We denote that

$$
\begin{aligned}
H_{ux}^{k} &= \frac{\partial^2\left(g+\lambda^T f\right)}{\partial u \partial x}\left(x_k, u_k, \lambda_k\right);\\
H_{u}^{k} &= \left[\frac{\partial H}{\partial u}\left(x_k, u_k, \lambda_k\right)\right]^T;\\
H_{uu}^{k} &= \frac{\partial^2\left(g+\lambda^T f\right)}{\partial u^2}\left(x_k, u_k, \lambda_k\right);\\
H_{x}^{k} &= \left[\frac{\partial H}{\partial x}\left(x_k, u_k, \lambda_k\right)\right]^T;\\
H_{xx}^{k} &= \frac{\partial^2\left(g+\lambda^T f\right)}{\partial x^2}\left(x_k, u_k, \lambda_k\right);\\
f_{u}^{k} &= \frac{\partial f}{\partial u}\left(x_k, u_k\right);\\
H_{xu}^{k} &= \frac{\partial^2\left(g+\lambda^T f\right)}{\partial x \partial u}\left(x_k, u_k, \lambda_k\right);\\
f_{x}^{k} &= \frac{\partial f}{\partial x}\left(x_k, u_k\right);\\
g_{u}^{k} &= \left[\frac{\partial g}{\partial u}\left(x_k, u_k\right)\right]^T;\\
g_{x}^{k} &= \left[\frac{\partial g}{\partial x}\left(x_k, u_k\right)\right]^T.
\end{aligned}
\tag{18}
$$

The first-order Taylor expansion of (15) on the old reference trajectory $[x_k \;\; u_k \;\; \lambda_k]^T$ is

$$
\begin{aligned}
\left[\frac{\partial H}{\partial u}\right]^T &\approx H_u^k + H_{ux}^k \Delta x + H_{uu}^k \Delta u + \left(f_u^k\right)^T \Delta\lambda,\\
\dot{\lambda} &\approx -H_x^k - H_{xx}^k \Delta x - H_{xu}^k\left(x_k, u_k, \lambda_k\right)\Delta u - \left(f_x^k\right)^T \Delta\lambda,\\
\dot{x} &\approx f\left(x_k, u_k\right) + f_x^k \Delta x + f_u^k \Delta u.
\end{aligned}
\tag{19}
$$

The following equations are established:

$$
\begin{aligned}
H_u^k + \left(f_u^k\right)^T \Delta\lambda &= g_u^k + \left(f_u^k\right)^T \lambda,\\
H_x^k + \left(f_x^k\right)^T \Delta\lambda &= g_x^k + \left(f_x^k\right)^T \lambda.
\end{aligned}
\tag{20}
$$

Substituting (20) into (19) yields

$$
\begin{aligned}
\dot{\lambda} &= -g_x^k - H_{xx}^k \Delta x - H_{xu}^k\left(x_k, u_k, \lambda_k\right)\Delta u - \left(f_x^k\right)^T \lambda,\\
\Delta\dot{x} &= f_x^k \Delta x + f_u^k \Delta u - \dot{x}_k + f\left(x_k, u_k\right),\\
g_u^k + H_{ux}^k \Delta x + H_{uu}^k \Delta u + \left(f_u^k\right)^T \lambda &= 0,\\
\Delta x\left(Ec_k\right) + \Delta x_k\left(Ec_k\right) &= xc_k,\\
\frac{\partial W}{\partial x\left(E_f\right)}\Delta x\left(E_f\right) + W\left(x_k\left(E_f\right)\right) &= 0,\\
\lambda\left(E_f\right) &= \left[\frac{\partial \phi}{\partial x\left(E_f\right)}\right]^T + \left[\varpi^T \frac{\partial W}{\partial x\left(E_f\right)}\right]^T.
\end{aligned}
\tag{21}
$$

This equation is a linear TPBVP about the variables $[\Delta x \;\; \Delta u \;\; \lambda]^T$. The linear TPBVP is solved using the Simpson rules in Section 6.

3.2. Backtracking Line Search for the Step Size. In this section, the step size l_k is determined by backtracking line search considering the solution of the linear TPBVP as the search direction. The penalty function for problem (13) is given by

$$
\begin{aligned}
p_k = J(x,u) + \eta\Bigg\{&\left\|W\left(x_f\right)\right\| + \int_{Ec_k}^{E_f}\left\|f(x,u) - \dot{x}\right\|\\
&+ \left\|x\left(Ec_k\right) - xc_k\right\|\Bigg\},
\end{aligned}
\tag{22}
$$

where η is the penalty parameter satisfied $\eta > \max|\lambda|$. We denote

$$y = \begin{bmatrix} x_k \\ u_k \end{bmatrix}, \qquad d_k = \begin{bmatrix} \Delta x \\ \Delta u \end{bmatrix}, \tag{23}$$

where $[\Delta x \ \ \Delta u \ \ \lambda]^T$ is the solution of the linear TPBVP (21).

The minimizer of penalty function $p_k(x,u)$ corresponds to the solution of problem (11). Backtracking line search was used for large-scale nonlinear optimization problems in [31]. The step size l_k is determined by backtracking line search that satisfies

$$\begin{aligned} l_k = \ & \max\{l \in S : p_{k+1}(y_k + l d_k) \\ & \leq p_{k+1}(y_k) + l\varepsilon_1 \delta p_{k+1}(y_k, d_k)\}, \\ S = \ & \{l : l = \varepsilon_2{}^m, m = 0, 1, 2, \ldots\}, \end{aligned} \tag{24}$$

where $\varepsilon_1 \in (0,1)$, $\varepsilon_2 \in (0,1)$, and $\delta p_{k+1}(y_k, d_k)$ is the variational of the functional $p_{k+1}(y)$ caused by variational d_k of y on y_k. Considering d_k as the solution of (21), $\delta p_{k+1}(y_k, d_k) \leq 0$ is established. The new state and guidance command of the reference trajectory are generated as follows:

$$\begin{bmatrix} x_{k+1} \\ u_{k+1} \end{bmatrix} = \begin{bmatrix} x_k \\ u_k \end{bmatrix} + l_k \begin{bmatrix} \Delta x \\ \Delta u \end{bmatrix}. \tag{25}$$

4. The Global Convergence of the Algorithm

In [32, 33], the convergence of the off-board algorithm was analyzed. But the relationship between the global convergence and the guidance cycle τ has not been discussed for on-board optimization in the previous literatures. In this section, we state and prove the global convergence of the on-board algorithm proposed in the preceding section. The solution sequence $[x_k \ \ u_k]^T$ generated by the algorithm will converge to the solution of the feedback optimal control problem. Unlike off-board trajectory optimization, the initial condition of the feedback optimal control problem depends on the current state of the vehicle in real time. For the kth guidance cycle, the optimal feedback control problem is described as (13). The penalty function p_k for this feedback optimal control problem is given by (22). For the subsequent guidance cycle, the optimal feedback guidance problem is given by

$$\begin{aligned} \min \quad & J = W\left(x\left(E_f\right)\right) + \int_{Ec_{k+1}}^{E_f} g(x,u)\, dE, \\ \text{s.t.} \quad & \dot{x} = f(x,u), \\ & x\left(Ec_{k+1}\right) = xc_{k+1}, \\ & W\left(x\left(E_f\right)\right) = 0, \end{aligned} \tag{26}$$

where

$$Ec_{k+1} = Ec_k + \int_{\tau_k}^{\tau_k + \Delta\tau} \frac{dE}{d\tau} d\tau, \tag{27}$$

$\Delta\tau$ is the guidance cycle and xc_{k+1} is the new state of vehicle from navigation system at the time $\tau_k + \Delta\tau$. The penalty function for optimal problem (24) is given by

$$\begin{aligned} p_{k+1}(x,u) = \ & J(x,u) + \eta \left\| W\left(x_k\left(E_f\right)\right)\right\| \\ & + \eta \int_{Ec_{k+1}}^{E_f} \left\| f(x,u) - \dot{x}\right\| dE \\ & + \eta \left\| x\left(Ec_{k+1}\right) - xc_{k+1}\right\|. \end{aligned} \tag{28}$$

We define the entire penalty function as follows:

$$\begin{aligned} \widetilde{p}_k(x,u) = \ & p_k(x,u) \\ & + \sum_{i=0}^{k-1} \int_{Ec_i}^{Ec_{i+1}} \left[\eta \left\| f(x_i,u_i) - \dot{x}_i\right\| + g(x_i,u_i)\right] dE. \end{aligned} \tag{29}$$

The entire penalty function $\widetilde{p}_k(x,u)$ includes the penalty function on the whole integration interval $[E_0, E_f]$.

Theorem 1. *If the minimizer of $\widetilde{p}_k(x_k,u_k)$ is exited, $g(x,u) \geq 0$, and $\Delta\tau$ is selected and satisfies*

$$\frac{\eta \left\| xc_{k+1} - xc_k - \int_{Ec_k}^{Ec_{k+1}} \dot{x}_k dE\right\|}{-\delta p_{k+1}(y_k, d_k)} < l_k \varepsilon_3, \tag{30}$$

where $\varepsilon_3 \in (0, \varepsilon_1)$. The solution sequence $[x_k \ \ u_k]^T$ generated from (24) will converge to the solution of the feedback optimal control problem.

Proof. From (22), (28), (29) and

$$x_k\left(Ec_{k+1}\right) = x_k\left(Ec_k\right) + \int_{Ec_k}^{Ec_{k+1}} \dot{x}_k dE \tag{31}$$

we can obtain that

$$\begin{aligned} & \widetilde{p}_{k+1}(x_k,u_k) - \widetilde{p}_k(x_k,u_k) \\ & = \eta \left\| x_k\left(Ec_k\right) - xc_k \right. \\ & \qquad \left. - \left(xc_{k+1} - xc_k - \int_{Ec_k}^{Ec_{k+1}} \dot{x}_k dE\right)\right\| \\ & \quad - \eta \left\| x_k\left(Ec_k\right) - xc_k\right\|. \end{aligned} \tag{32}$$

From (32), we obtain

$$\begin{aligned}
&\lim_{\Delta\tau\to 0}\left[\widetilde{p}_{k+1}\left(x_k,u_k\right)-\widetilde{p}_k\left(x_k,u_k\right)\right]=0,\\
&\lim_{f(x_k,u_k)-\dot{x}_k\to 0}\left[\widetilde{p}_{k+1}\left(x_k,u_k\right)-\widetilde{p}_k\left(x_k,u_k\right)\right]=0,
\end{aligned} \tag{33}$$

$$\begin{aligned}
&\widetilde{p}_{k+1}\left(x_k,u_k\right)-\widetilde{p}_k\left(x_k,u_k\right)\\
&\quad=\eta\left\{\left\|x_k\left(Ec_k\right)-xc_{k+1}+\int_{Ec_k}^{Ec_{k+1}}\dot{x}_k dE\right\|\right.\\
&\qquad\left.-\left\|x_k\left(Ec_k\right)-xc_k\right\|\right\}\\
&\quad\le\eta\left\{\left\|x_k\left(Ec_k\right)-xc_k\right\|\right.\\
&\qquad+\left\|xc_{k+1}-xc_k-\int_{Ec_k}^{Ec_{k+1}}\dot{x}_k dE\right\|\\
&\qquad\left.-\left\|x_k\left(Ec_k\right)-xc_k\right\|\right\}\\
&\quad=\eta\left\|xc_{k+1}-xc_k-\int_{Ec_k}^{Ec_{k+1}}\dot{x}_k dE\right\|.
\end{aligned} \tag{34}$$

From conditions (24) and (30), it is obtained that

$$\begin{aligned}
&\widetilde{p}_{k+1}\left(x_{k+1},u_{k+1}\right)\\
&\quad\le\widetilde{p}_{k+1}\left(x_k,u_k\right)+l_k\varepsilon_1\delta p_{k+1}\left(d_k\right)\\
&\quad=\widetilde{p}_k\left(x_k,u_k\right)+l_k\varepsilon_1\delta p_{k+1}\left(d_k\right)\\
&\qquad+\eta\left\{\left\|x_k\left(Ec_k\right)-xc_k\right.\right.\\
&\qquad\qquad\left.-\left(xc_{k+1}-xc_k-\int_{Ec_k}^{Ec_{k+1}}\dot{x}_k dE\right)\right\|\\
&\qquad\qquad\left.-\left\|x_k\left(Ec_k\right)-xc_k\right\|\right\}\\
&\quad\le\widetilde{p}_k\left(x_k,u_k\right)+\eta\left\|xc_{k+1}-xc_k-\int_{Ec_k}^{Ec_{k+1}}\dot{x}_k dE\right\|\\
&\qquad+l_k\varepsilon_1\delta p_{k+1}\left(y_k,d_k\right)\\
&\quad\le\widetilde{p}_k\left(x_k,u_k\right)+\eta\left\|xc_{k+1}-xc_k-\int_{Ec_k}^{Ec_{k+1}}\dot{x}_k dE\right\|\\
&\qquad+l_k\varepsilon_3\delta p_{k+1}\left(y_k,d_k\right)\\
&\quad<\widetilde{p}_k\left(x_k,u_k\right).
\end{aligned} \tag{35}$$

Thus, the sequence $\widetilde{p}_k(x_k,u_k)$, $k=1,2,3,\ldots$. is monotonically decreasing. Considering the existence of a minimizer, $\widetilde{p}_k(x_k,u_k)$ converges. Thus, the following equation is established:

$$\lim_{k\to\infty}\left(l_k\varepsilon_3\delta p_{k+1}\left(y_k,d_k\right)-l_k\varepsilon_1\delta p_{k+1}\left(y_k,d_k\right)\right)=0. \tag{36}$$

From (36), we derive

$$\lim_{k\to\infty}\left(l_k\delta p_{k+1}\left(y_k,d_k\right)\right)=0. \tag{37}$$

If $d_k\neq 0$, $[x_k\ \ u_k]^T$ is not the minimizer of penalty function, then $\delta p_{k+1}(y_k,d_k)\neq 0$. Considering that l_k is bounded away from zero, we derive

$$\begin{aligned}
&\lim_{k\to\infty}d_k=0,\\
&\lim_{k\to\infty}\delta p_{k+1}\left(y_k,d_k\right)=0,\\
&\lim_{k\to\infty}\left[\dot{x}_k-f\left(x_k,u_k\right)\right]=0,\\
&\lim_{k\to\infty}\left(\dot{\lambda}_k+H_x^k\right)=0,\\
&\lim_{k\to\infty}H_u^k=0.
\end{aligned} \tag{38}$$

Thus, the solution sequence $[x_k\ \ u_k]^T$ generated by the algorithm will converge to the solution of the optimal control problem. □

5. Smooth Approximation for Inequality Constraints

The nondifferentiable TPBVP from optimal control problem (11) with the inequality constraints brings difficulties for the proposed algorithm, which can only solve a smooth problem. Smooth approximations for nondifferentiable optimization problems have been studied in [5, 6, 34]. In this section we introduce the smooth approximation method for the inequality constraints. If the inequality constraint function is about the state and the guidance command

$$C\left(x,u\right)\le 0 \tag{39}$$

the Hamiltonian for the optimal control problem (11) with inequality constraints (39) is given by

$$H=g\left(x,u\right)+\lambda^T f\left(x,u\right)+\mu\max\left\{C\left(x,u\right),0\right\}. \tag{40}$$

However, the Hamiltonian (40) is a nondifferentiable function, which brings difficulty for the proposed algorithm. For the smooth Hamiltonian approximation, a differentiable function is substituted for $\max\{C(x,u),0\}$. We denote the nondifferentiable function as follows:

$$\max\left\{0,y\right\}=\int_{-\infty}^{y}w\left(z\right)dz, \tag{41}$$

where $w(z)$ is the step function

$$w\left(z\right)=\begin{cases}1, & \text{if } z\ge 0,\\ 0, & \text{if } z<0.\end{cases} \tag{42}$$

Considering $s(z,a)$ as the approximation function of $w(z)$, the differentiable approximation to $\max\{0,y\}$ is obtained as

$$f_p\left(y,a\right)\approx\int_{-\infty}^{y}s\left(z,a\right)dz=y+\frac{1}{a}\ln\left(1+e^{-ay}\right), \tag{43}$$

where $s(z,a)$ is Sigmoid function

$$s(z,a) = \frac{1}{1+e^{-az}}, \quad a > 0. \tag{44}$$

The Properties of $f_p(y,a)$, $a > 0$ are as follows [5]:

(1) $f_p(y,a)$ is n-times continuously differentiable for any positive integer n, with $\partial f_p(y,a)/\partial y = 1/(1+e^{-ay})$ and $\partial^2 f_p(y,a)/\partial y^2 = ae^{-ay}/(1+e^{-ay})^2$.

(2) $f_p(y,a)$ is strictly convex and strictly increasing on $\mathbb{R}$.

(3) $f_p(y,a) > \max\{0, y\}$.

(4) $\lim_{a\to\infty} f_p(y,a) = \max\{0, y\}$.

(5) $f_p(y,a) > f_p(y,a_1)$ for $a < a_1$, $y \in \mathbb{R}$.

Substituting (43) into (40), the following differentiable Hamiltonian approximation is obtained:

$$\widehat{H} = g(x,u) + \lambda^T f(x,u) + \mu\left[C + \frac{1}{a}\operatorname{In}\left(1+e^{-aC}\right)\right]. \tag{45}$$

If the inequality constraint function is a qth-order state variable inequality constraint given by

$$C(x) \le 0. \tag{46}$$

If p times derivatives of $C(x)$ are required before u appears explicitly in the result, the Hamiltonian with inequality constraints (46) is given by

$$H = g(x,u) + \lambda^T f(x,u) + \mu C^{(q)}, \tag{47}$$

where

$$\mu = 0 \quad \text{if } C < 0. \tag{48}$$

Considering the differentiable approximation to μ as follows:

$$\mu = \widehat{\mu} w(C) \approx \widehat{\mu}\frac{1}{1+e^{-aC}} \tag{49}$$

the following differentiable Hamiltonian approximation is obtained:

$$\widehat{H} = g(x,u) + \lambda^T f(x,u) + \widehat{\mu}\frac{1}{1+e^{-aC}}C^{(q)}. \tag{50}$$

With the differentiable Hamiltonian approximation, the inequality constraints are considered in the proposed guidance algorithm.

6. Simulation Results

6.1. Numerical Calculation Based on Linear TPBVP Discretization. In this section, the linear TPVBP is transformed into linear equations using the Simpson rule, which corresponds to the three-point Newton-Cotes quadrature rule. The Simpson rule for differential equation $dX/dE = y(E)$ is given by

$$\int_a^b y(E)\,dE = \frac{b-a}{6}\left[y(a) + 4y\left(\frac{a+b}{2}\right) + y(b)\right]. \tag{51}$$

From (51), we obtain

$$X(b) - X(a) = \frac{b-a}{6}\left[y(a) + 4y\left(\frac{a+b}{2}\right) + y(b)\right]. \tag{52}$$

We disperse the normalized energy E into N equal segments as $[E_0 \;\; E_1 \;\; \cdots \;\; E_N]$, with $E_0 = Ec_k$ and $E_N = E_f$. The differential equation $dX/dE = y(X,E)$ can be transformed into the following equation:

$$\begin{aligned} &X(E_i) - X(E_{i-1}) \\ &= \frac{E_i - E_{i-1}}{6}\left[y(X_i, E_i)\right. \\ &\qquad + 4y\left(\frac{X_i + X_{i-1}}{2}, \frac{E_i + E_{i-1}}{2}\right) \\ &\qquad \left. + y(X_{i-1}, E_{i-1})\right], \quad i = 1, 2, 3, \ldots, N. \end{aligned} \tag{53}$$

Based on (53), the linear TPBVP (21) can be transformed into linear equations described by

$$AX = B. \tag{54}$$

The linear equations can be solved by Gaussian elimination.

Finally, we can obtain the solution $\Delta x(E)$, $\Delta u(E)$, and $\lambda(E)$ of the linear TPBVP (21) from the solution of the linear equations through interpolating.

6.2. GHV Model. The proposed method is applied to the Generic Hypersonic Vehicle (GHV) to verify the effectiveness by flight simulation. In order to develop a complete set of aerodynamic coefficients, experimental longitudinal and lateral-directional aerodynamics were obtained for the GHV by using six Langley wind tunnels [35]. The aerodynamic database of the GHV is shown in [35]. The GHV model with scramjet propulsion system is used for the simulation, where $S_{\text{ref}} = 334.73\ \text{m}^2$ and the full-scale weight $m_{\text{ini}} = 110000\ \text{kg}$.

According to the characterization of scramjet propulsion system described in [2, 27], the development of the propulsion system begins with the following equation:

$$T = 0.5\phi I_{\text{sp}}(\phi, M_a)\rho v g_0 C_T(\alpha, M_a), \tag{55}$$

where ϕ is the throttle command which varies from 0 to 1. The coefficient C_T depends on α and M_a as follows:

$$C_T = -0.0012M_a\alpha^2 + 0.008\alpha + 1.4 - 0.1M_a. \tag{56}$$

The impulse I_{sp} is given by the following equation:

$$I_{\text{sp}} = -81M_a^2 + 1004M_a - 52 + 100\phi. \tag{57}$$

6.3. Simulation Results for Modeling and Initial State Error. Considering the high cost of the flight experimental test, researchers do flight numerical simulation, hardware-in-the-loop simulation and final flight experimental test to verify the guidance algorithm step by step. In this section, flight

Table 1: Initial and required final states of the vehicle.

r_{ini} (m)	v_{ini} (m/s)	γ_{ini} (deg)	r_{rf} (m)	v_{rf} (m/s)	γ_{rf} (deg)
20000	1000	0	35000	2000	0

numerical simulation results for the GHV with modeling error and initial state error are given to show the effectiveness of the proposed guidance algorithm. For the modeling error caused by the wind tunnel experimental test, the aerodynamic coefficients bias is considered in the flight simulation. The simulations end once the final normalized energy E_f is reached. The optimal guidance algorithm updates the trajectory every guidance cycle, which is 0.3 s. The initial and required final states of the air-breathing vehicle are shown in Table 1. The number of the discrete nodes $N = 10$. The dynamic pressure inequality constraint is given by

$$Q = \frac{1}{2}\rho v^2 \leq 140000 \text{ Pa}. \tag{58}$$

To assess the capability of the proposed algorithm to deal with disturbance, the aerodynamic coefficients bias and the initial state error in the simulations are given by following cases:

(1) $\Delta C_L = -0.1C_L$, $\Delta C_D = +0.1C_D$.

(2) $\Delta C_L = -0.1C_L$, $\Delta C_D = +0.1C_D$, $\Delta r_{\text{ini}} = +500$ m.

(3) $\Delta C_L = -0.1C_L$, $\Delta C_D = +0.1C_D$, $\Delta r_{\text{ini}} = -500$ m.

(4) $\Delta C_L = -0.1C_L$, $\Delta C_D = +0.1C_D$, $\Delta r_{\text{ini}} = +1000$ m.

(5) $\Delta C_L = -0.1C_L$, $\Delta C_D = +0.1C_D$, $\Delta r_{\text{ini}} = -1000$ m.

The simulation results of the optimal guidance algorithm are shown in Figures 4, 5, 6, 7, and 8. The altitude, velocity, flight path angle, angle of attack, and dynamic pressure are, respectively, shown in Figures 4 to 8. As expected, the final state is achieved under aerodynamic bias and initial state error. Figure 8 shows that the state inequality constraint is satisfied. The dynamic pressure is less than 140000 Pa for different cases.

Table 2 shows the terminal error and the fuel cost of the optimal guidance algorithm. The terminal accuracy is high for different cases. Moreover, the fuel cost of the optimal guidance algorithm is lower than that of the tracking guidance algorithm. A greater initial state error will result in more fuel savings. In summary, with lower fuel cost the results of the proposed optimal guidance algorithm satisfies all the equality and inequality constraints. The simulation results show the great potential for the final flight experimental test.

7. Conclusion

In this paper, we present an optimal guidance algorithm for air-breathing launch vehicle based on optimal trajectory correction. The proposed guidance algorithm corrects the reference trajectory in every guidance cycle to satisfy the optimality condition of the optimal feedback control problem.

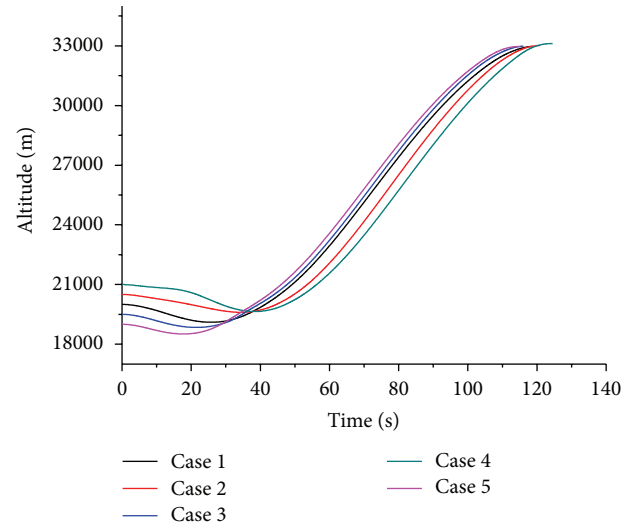

Figure 4: The altitude of the simulation results.

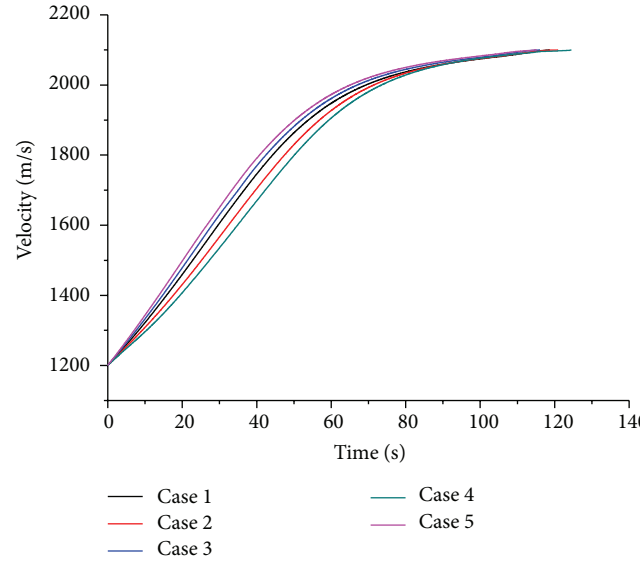

Figure 5: The velocity of the simulation results.

By linearizing the optimality condition, the linear TPBVP is obtained for optimal trajectory correction. The solution of the linear TPBVP is derived using the Simpson rule. The new trajectory is generated by a linear search for the step size of the solution. Smooth Hamiltonian approximation is implemented to the inequality constraints. The sufficiency condition for the global convergence of the guidance algorithm is given in this paper.

Finally, simulations for 5 different cases of modeling and initial state error are presented. Compared with the tracking guidance method, the simulation results prove the low fuel cost and high precision of the proposed optimal guidance method.

Table 2: The simulation results for optimal guidance algorithm.

Case	Δr_f (m)	Δv_f (m/s)	$\Delta \gamma_f$ (deg)	Fuel cost (kg)	Fuel cost (tracking method) (kg)
1	−28.20	0.136	0.20	4572.19	4574.62
2	8.59	−0.03	−0.15	4583.14	4628.39
3	−15.08	0.07	0.20	4584.74	4605.66
4	108.16	0.47	−0.23	4602.92	4776.00
5	−32.43	0.19	−0.16	4601.33	4688.94

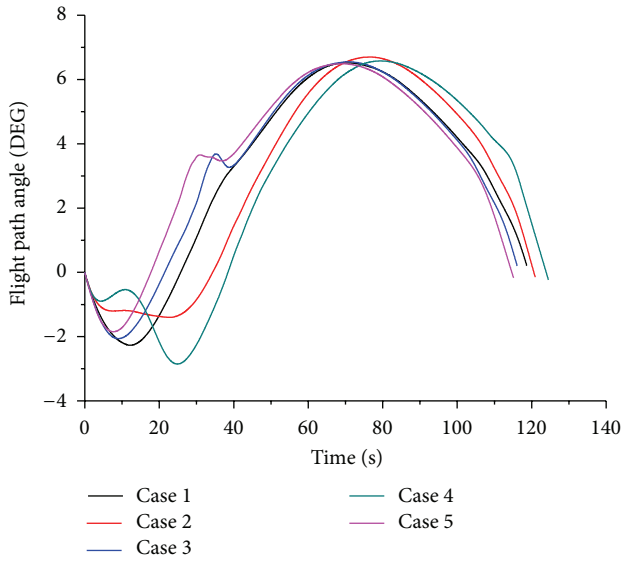

Figure 6: The flight path angle of the simulation results.

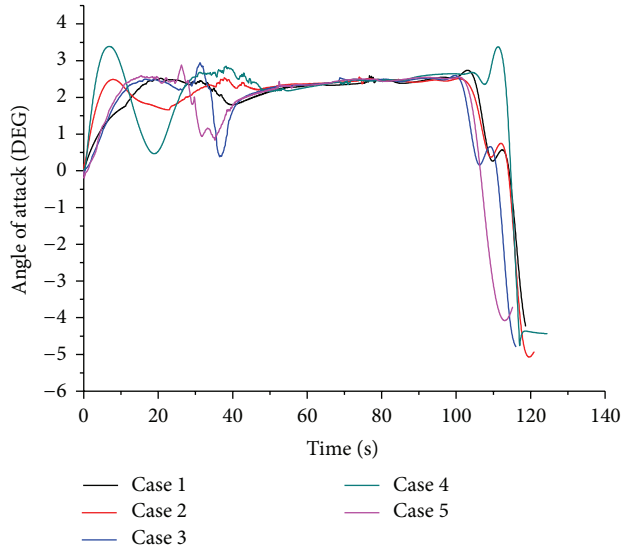

Figure 7: The angle of attack of the simulation results.

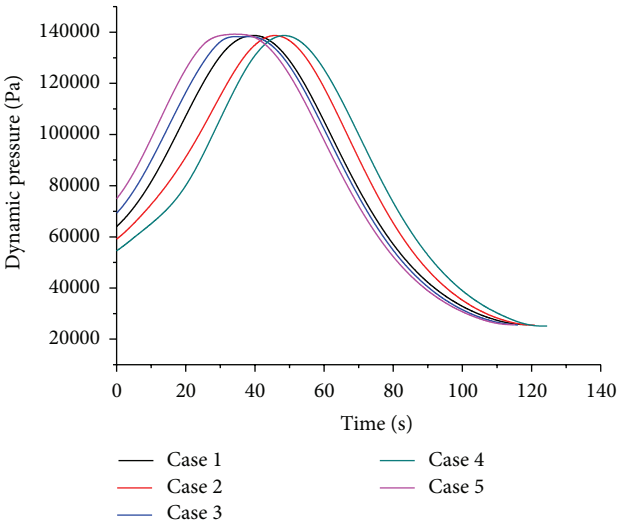

Figure 8: The dynamic pressure of the simulation results.

Acknowledgments

This work was supported in part by the National Nature Science Foundation of China nos. 61203081 and 61174079, Doctoral Fund of Ministry of Education of China no. 20120142120091, and Precision manufacturing technology and equipment for metal parts no. 2012DFG70640.

References

[1] H. J. Henry Jr. and C. H. McLellan, "Air-breathing launch vehicle for earth-orbit shuttle. New technology and development approach," *Journal of Aircraft*, vol. 8, no. 5, pp. 381–387, 1971.

[2] J. E. Corban, A. J. Calise, and G. A. Flandro, "Real-time guidance algorithm for aerospace plane optimal ascent to low earth orbit," in *Proceedings of the American Control Conference*, pp. 2475–2481, Pittsburgh, PA, USA, June 1989.

[3] C. H. Yam, D. D. Lorenzo, and D. Izzo, "Low-thrust trajectory design as a constrained global optimization problem," *Journal of Aerospace Engineering G*, vol. 225, no. 11, pp. 1243–1251, 2011.

[4] B. A. Conway, "A survey of methods available for the numerical optimization of continuous dynamic systems," *Journal of Optimization Theory and Applications*, vol. 152, no. 2, pp. 271–306, 2012.

[5] C. H. Chen and O. L. Mangasarian, "Smoothing methods for convex inequalities and linear complementarity problems," *Mathematical Programming*, vol. 71, no. 1, pp. 51–69, 1995.

[6] X. Chen, "Smoothing methods for nonsmooth, nonconvex minimization," *Mathematical Programming*, vol. 134, no. 1, pp. 71–99, 2012.

[7] W. Wang, Y. Shang, and Y. Zhang, "A filled function approach for nonsmooth constrained global optimization," *Mathematical*

Problems in Engineering, vol. 2010, Article ID 310391, 9 pages, 2010.

[8] L. I. Rozonoer, "Linear-quadratic optimization and some general hypotheses on optimal control," *Mathematical Problems in Engineering*, vol. 5, no. 4, pp. 275–289, 1999.

[9] J. T. Betts, "Survey of numerical methods for trajectory optimization," *Journal of Guidance, Control, and Dynamics*, vol. 21, no. 2, pp. 193–207, 1998.

[10] G. Q. Huang, Y. P. Lu, and Y. Nan, "A survey of numerical algorithms for trajectory optimization of flight vehicles," *Science China-Technological Sciences*, vol. 55, no. 9, pp. 2538–2560, 2012.

[11] Y. Ulybyshev, "Discrete pseudocontrol sets for optimal control problems," *Journal of Guidance, Control, and Dynamics*, vol. 33, no. 4, pp. 1133–1142, 2010.

[12] M. Vasile and F. Zuiani, "Multi-agent collaborative search: an agent-based memetic multi-objective optimization algorithm applied to space trajectory design," *Journal of Aerospace Engineering G*, vol. 225, no. 11, pp. 1211–1227, 2011.

[13] M. Pontani and B. A. Conway, "Particle swarm optimization applied to space trajectories," *Journal of Guidance, Control, and Dynamics*, vol. 33, no. 5, pp. 1429–1441, 2010.

[14] Y. P. Ulybyshev, "Optimization of low-thrust orbit transfers with constraints," *Cosmic Research*, vol. 50, no. 5, pp. 376–390, 2012.

[15] M. Chen, R. Mei, and B. Jiang, "Sliding mode control for a class of uncertain MIMO nonlinear systems with application to near-space vehicles," *Mathematical Problems in Engineering*, vol. 2013, Article ID 180589, 9 pages, 2013.

[16] H. Zhang, Y. Shi, M. Q. Xu, and H. T. Cui, "Observer-based tracking controller design for networked predictive control systems with uncertain markov delays," in *Proceedings of the American Control Conference*, pp. 5682–5687, 2012.

[17] H. Zhang and Y. Shi, "Robust H-infinity sliding-mode control for markovian jump systems subject to intermittent observations and partially known transition probabilities," *Systems & Control Letters*, vol. 62, no. 12, pp. 1114–1124, 2013.

[18] Z. Shuai, H. Zhang, J. Wang, J. Li, and M. Ouyang, "Combined AFS and DYC control of four-wheel-independent-drive electric vehicles over CAN network with time-varying delays," *IEEE Transactions on Vehicular Technology*, no. 99, p. 1, 2013.

[19] H. Zhang, Y. Shi, and A. Saadat Mehr, "Robust static output feedback control and remote PID design for networked motor systems," *IEEE Transactions on Industrial Electronics*, vol. 58, no. 12, pp. 5396–5405, 2011.

[20] H. Zhang, Y. Shi, and M. X. Liu, "H-infinity step tracking control for networked discrete-time nonlinear systems with integral and predictive actions," *IEEE Transactions on Industrial Informatics*, vol. 9, no. 1, pp. 337–345, 2013.

[21] X. J. Wang and S. P. Wang, "Adaptive fuzzy robust control for a class of nonlinear systems via small gain theorem," *Mathematical Problems in Engineering*, vol. 2013, Article ID 201432, 11 pages, 2013.

[22] V. Brinda, S. Dasgupta, and M. Lal, "Trajectory optimization and guidance of an air breathing hypersonic vehicle," in *Proceedings of the 14th AIAA/AHI International Space Planes and Hypersonics Systems Technologies Conference*, vol. 2, pp. 856–869, November 2006.

[23] B. Tian and Q. Zong, "Optimal guidance for reentry vehicles based on indirect legendre pseudospectral method," *Acta Astronautica*, vol. 68, no. 7-8, pp. 1176–1184, 2011.

[24] M. H. Gräßlin, J. Telaar, and U. M. Schöttle, "Ascent and reentry guidance concept based on NLP-methods," *Acta Astronautica*, vol. 55, no. 3–9, pp. 461–471, 2004.

[25] P. Lu and B. Pan, "Highly constrained optimal launch ascent guidance," *Journal of Guidance, Control, and Dynamics*, vol. 33, no. 2, pp. 404–414, 2010.

[26] P. Lu, H. Sun, and B. Tsai, "Closed-loop endo-atmospheric ascent guidance," in *Proceedings of the AIAA Guidance, Navigation, and Control Conference*, Monterey, Calif, USA, 2002.

[27] J. Oscar Murillo and P. Lu, "Fast ascent trajectory optimization for hypersonic air-breathing vehicles," in *Proceedings of the AIAA Guidance, Navigation, and Control Conference*, pp. 5–8, Toronto, Canada, 2010.

[28] M. Marrdonny and M. Mobed, "A guidance algorithm for launch to equatorial orbit," *Aircraft Engineering and Aerospace Technology*, vol. 81, no. 2, pp. 137–148, 2009.

[29] T. Yamamoto and J. Kawaguchi, "A new real-time guidance strategy for aerodynamic ascent flight," *Acta Astronautica*, vol. 61, no. 11-12, pp. 965–977, 2007.

[30] C. Filici and R. S. Sánchez Peña, "Online guidance updates using neural networks," *Acta Astronautica*, vol. 66, no. 3-4, pp. 477–485, 2010.

[31] P. T. Boggs, A. J. Kearsley, and J. W. Tolle, "A global convergence analysis of an algorithm for large-scale nonlinear optimization problems," *SIAM Journal on Optimization*, vol. 9, no. 4, pp. 833–862, 1999.

[32] S. Schlenkrich and A. Walther, "Global convergence of quasi-Newton methods based on adjoint Broyden updates," *Applied Numerical Mathematics*, vol. 59, no. 5, pp. 1120–1136, 2009.

[33] S. Schlenkrich, A. Griewank, and A. Walther, "On the local convergence of adjoint Broyden methods," *Mathematical Programming*, vol. 121, no. 2, pp. 221–247, 2010.

[34] S. Lian and L. Zhang, "A simple smooth exact penalty function for smooth optimization problem," *Journal of Systems Science & Complexity*, vol. 25, no. 3, pp. 521–528, 2012.

[35] S. Keshmiri, R. Colgren, and M. Mirmirani, "Development of an aerodynamic database for a generic hypersonic air vehicle," in *Proceedings of the AIAA Guidance, Navigation, and Control Conference*, pp. 3978–3998, San Francisco, Calif, USA, August 2005.